New calculation of the geo-neutrino energy spectrum and its implication

Yu-Feng Li
Institute of High Energy Physics, Beijing
liyufeng@ihep.ac.cn

3rd IAEA TM on Nuclear Data Needs for Antineutrino Spectra
7-11 April 2025, Seoul

Based on arXiv: 2412.07711 [YFL, Xin]

Introduction

1. Geoneutrino spectrum is the basis for geoneutrino sensitivity study

2. Current flux : Enomoto's model
   - ENSDF 2005 ⇒ ENSDF 2023
   - Single beta branch
     - Only allowed transition
     - Without high-order corrections ⇒ Should be included

Geoneutrino flux —IBD cross section→ Predicted signals (rate and shape)

3. Spectral impact to analysis

   Observed data: KamLAND (2022), Borexino (2020)

   Predicted data: JUNO

Geoneutrinos: Introduction

Geoneutrino

- The intersection of particle physics and geophysics
- An independent method to study the matter composition deep within the Earth

Abundance of the radioactive elements → Radiogenic heat

$$^{238}\mathrm{U} \rightarrow {}^{206}\mathrm{Pb} + 8\alpha + 6e^- + 6\bar{\nu}_e + 51.698\ \mathrm{MeV}$$
$$^{235}\mathrm{U} \rightarrow {}^{207}\mathrm{Pb} + 7\alpha + 4e^- + 4\bar{\nu}_e + 46.402\ \mathrm{MeV}$$
$$^{232}\mathrm{Th} \rightarrow {}^{208}\mathrm{Pb} + 6\alpha + 4e^- + 4\bar{\nu}_e + 42.652\ \mathrm{MeV}$$
$$^{40}\mathrm{K} \rightarrow {}^{40}\mathrm{Ca} + e^- + \bar{\nu}_e + 1.311\ \mathrm{MeV}$$
$$^{40}\mathrm{K} + e^- \rightarrow {}^{40}\mathrm{Ar} + \nu_e + 1.505\ \mathrm{MeV}$$

Geo-neutrino flux → Radiogenic heat

$$S_{\mathrm{Total}} = S_{\mathrm{Crust}} + S_{\mathrm{CLM}} + S_{\mathrm{Mantle}}$$

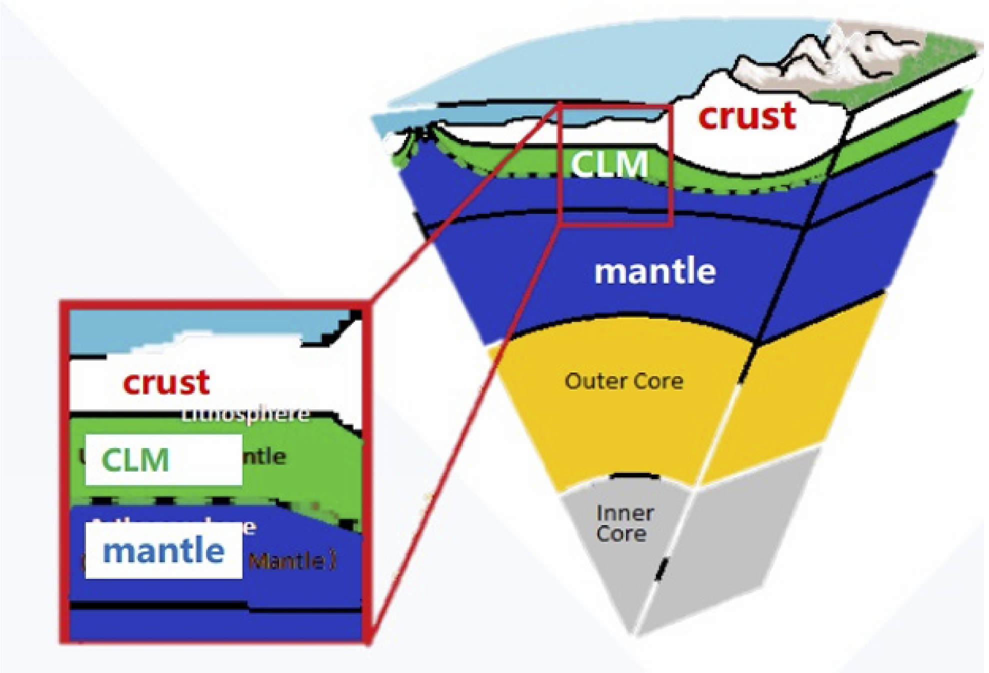

- Crust: high U & Th
- CLM (Continental Lithospheric Mantle): relatively low U & Th
- Mantle: very low U & Th, large volume

Geoneutrinos: Introduction

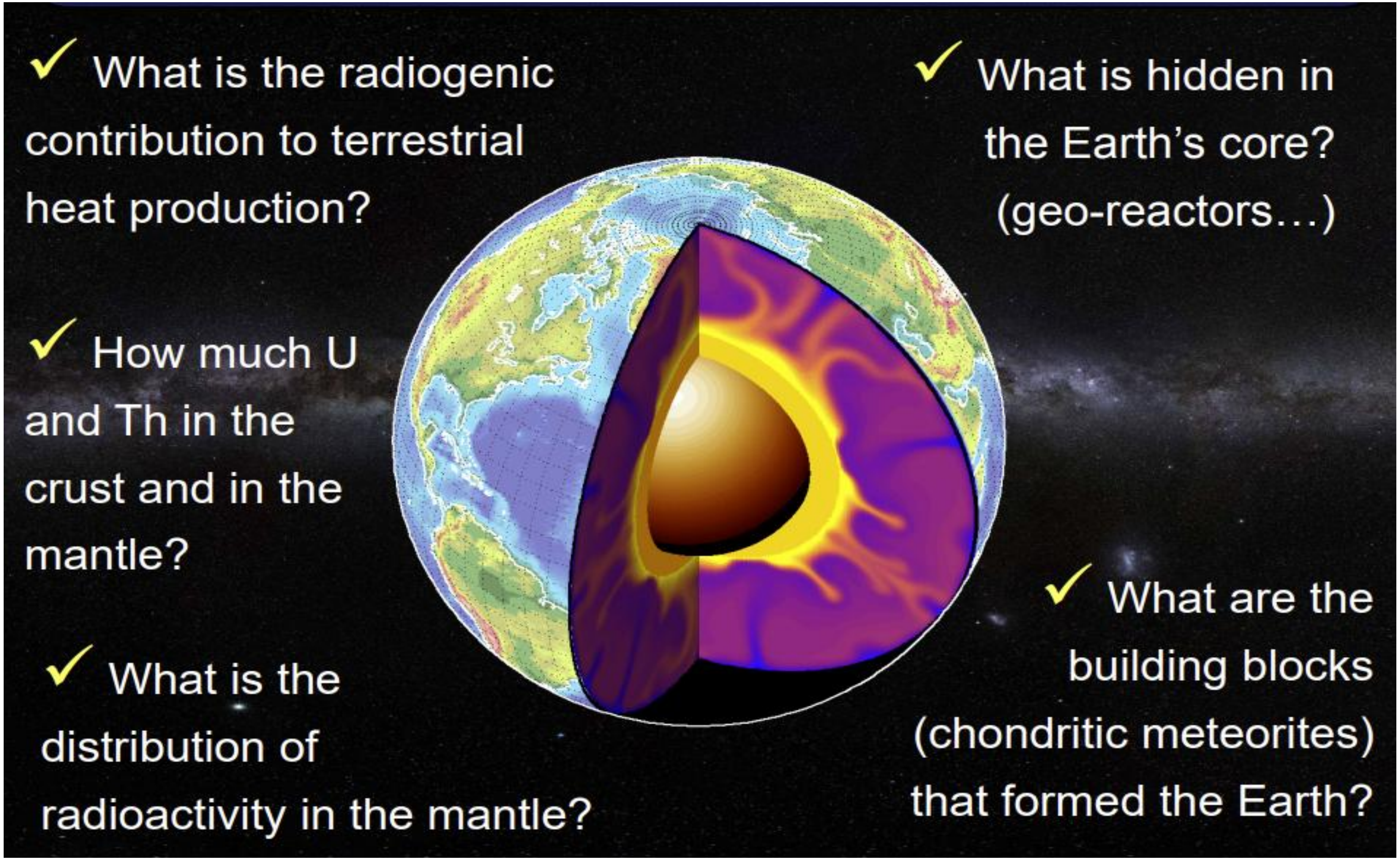

From Mantovani

Geoneutrino Observation

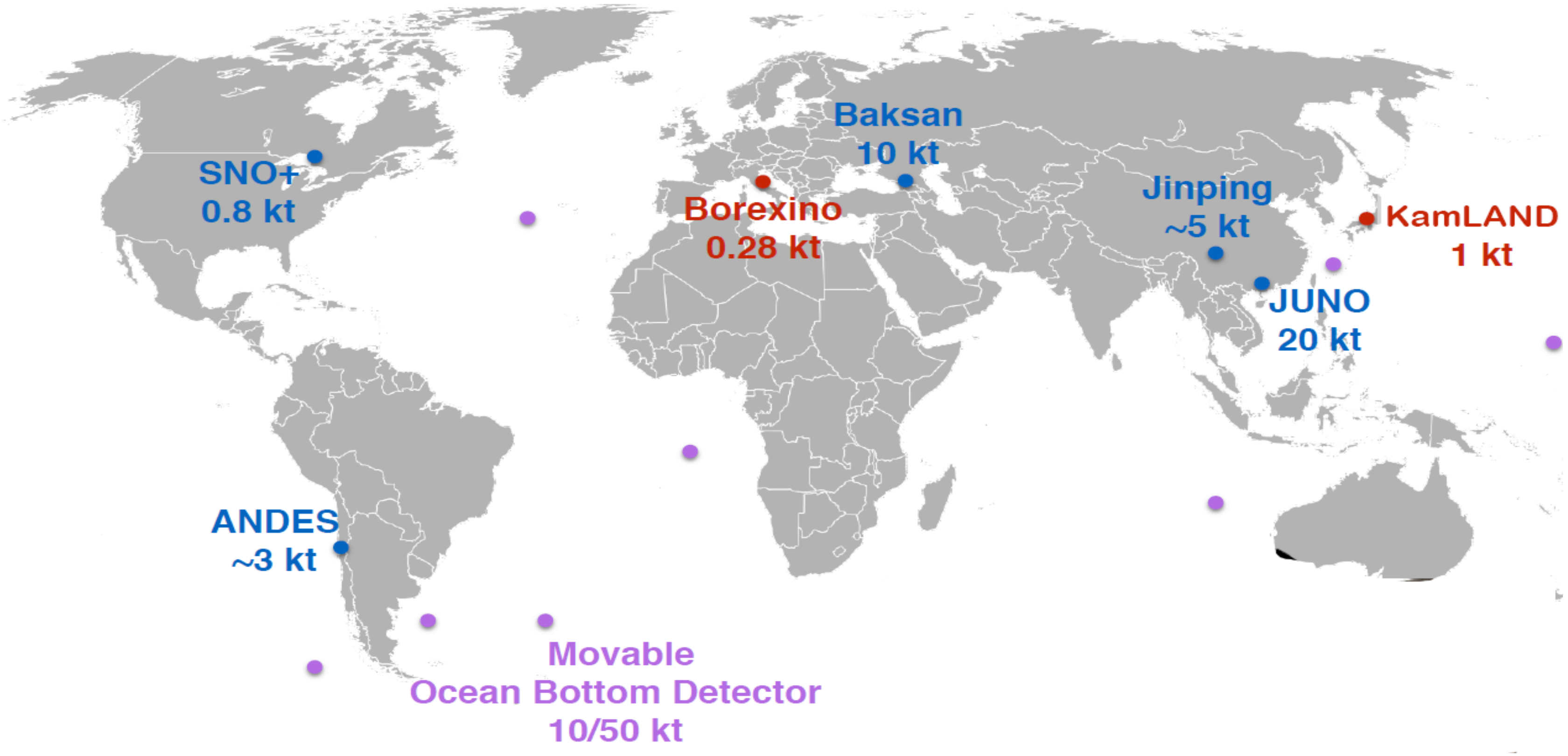

Observation in KamLAND & Borexino

KamLAND (2022)

- Liquid scintillator of 1 kon
- 18 years ~ 170 geo-neutrinos
- Precision
  - ~ 36% for ^{238}U
  - ~ 53% for ^{232}Th

Geophysical Research Letters, 49, e2022GL099566

Borexino (2020)

- Liquid scintillator of 0.3 kon
- 10 years ~ 50 geo-neutrinos
- Precision
  - ~ 53% for ^{238}U
  - ~ 55% for ^{232}Th

Phys. Rev. D 101, 012009 (2020)

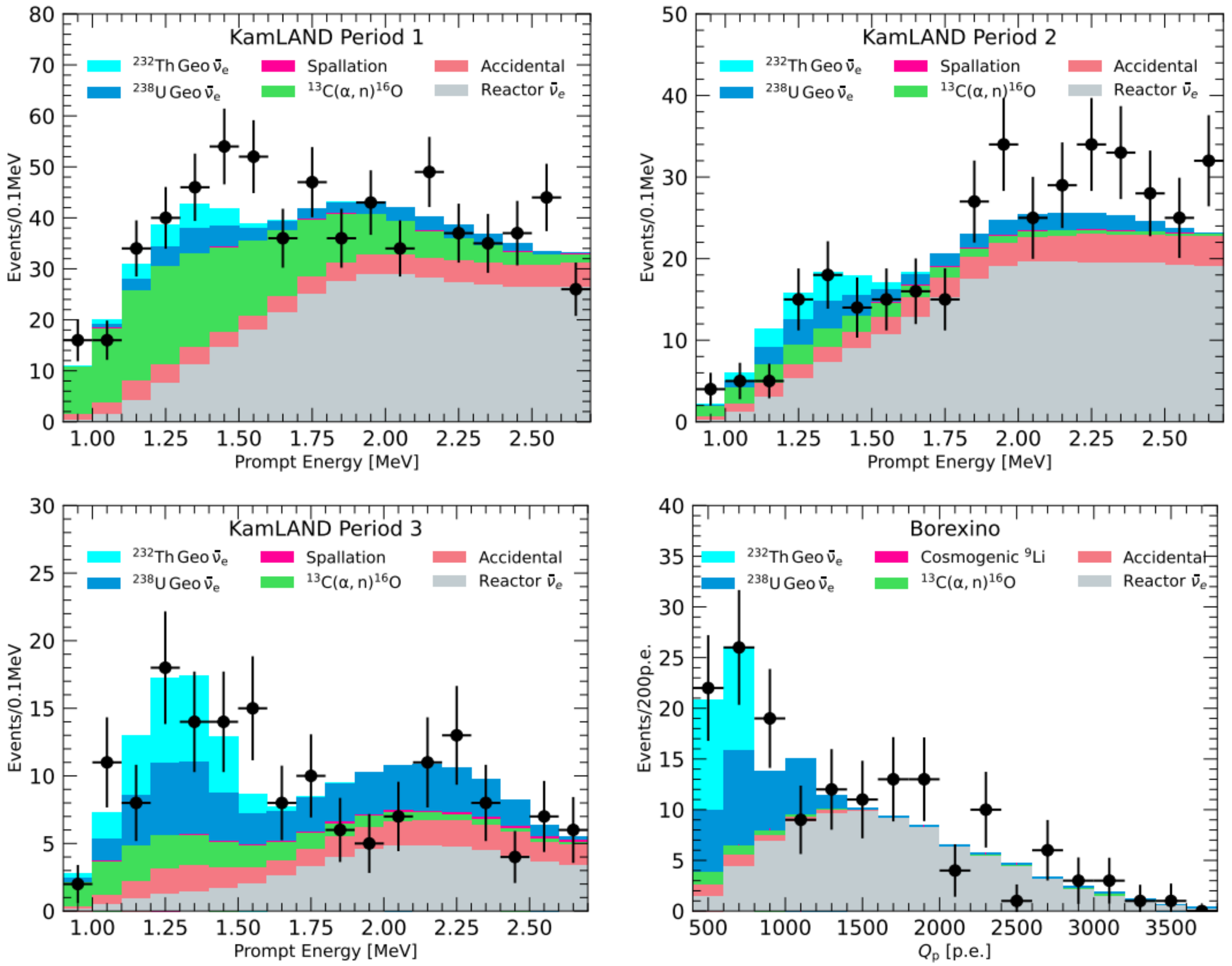

Motivation for precise spectral calculation

- Liquid scintillator detectors lack of directionality

→The energy spectral feature of both geoneutrinos and reactor neutrinos is important !

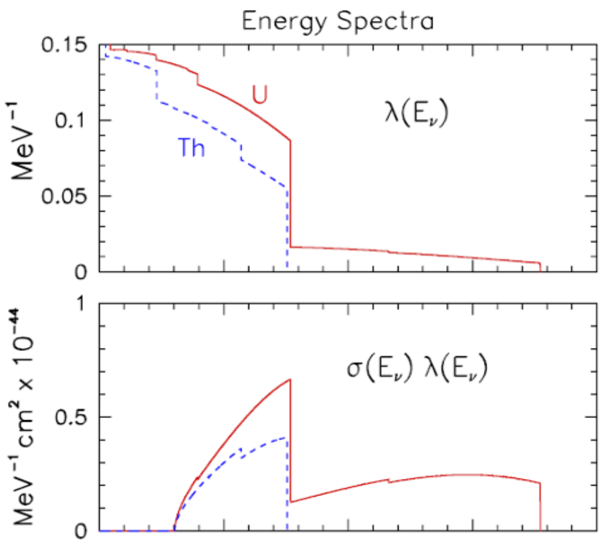

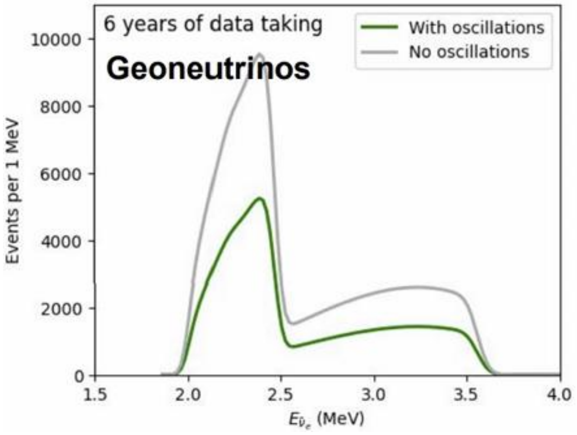

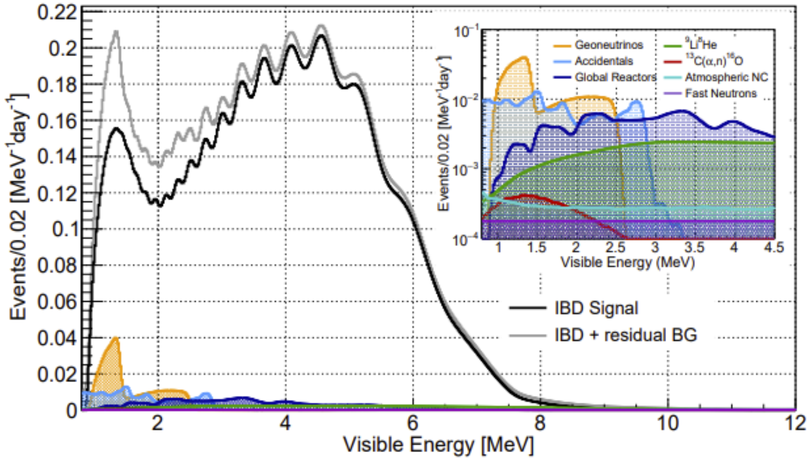

JUNO collaboration, 2204.13249

The new geoneutrino flux model

(Li & Xin, arXiv: 2412.07711):

Summation model with latest database,
higher order corrections and forbidden decays

Geo-neutrino flux: the new calculation

A single decay branch
Fermi's golden rule
(modern calculation)

Normalization — Fermi function — Shape factor — Corrections

$$S_{\bar{\nu}}^{k}(E_{\bar{\nu}}) = K\, p_{\bar{\nu}} E_{\bar{\nu}} (E_0^k - E_{\bar{\nu}})^2\, F(Z, E_{\bar{\nu}})\, C(E_{\bar{\nu}})\, [1 + \delta_{\bar{\nu}}(Z, A, E_{\bar{\nu}})]$$

- radiative corrections
- weak magnetism
- finite size

Decay chain for ^{232}Th

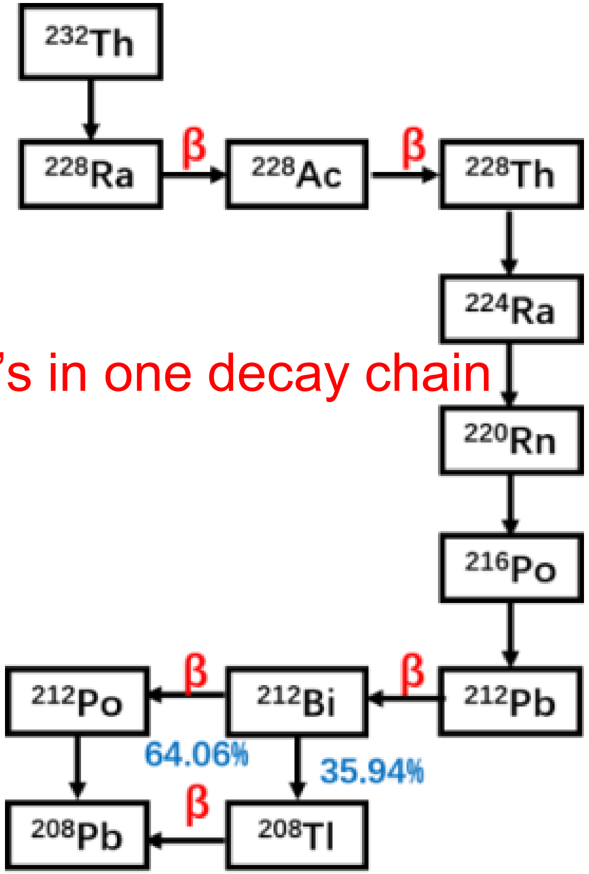

4 $\bar{\nu}_e$'s in one decay chain

Decay chain for ^{238}U

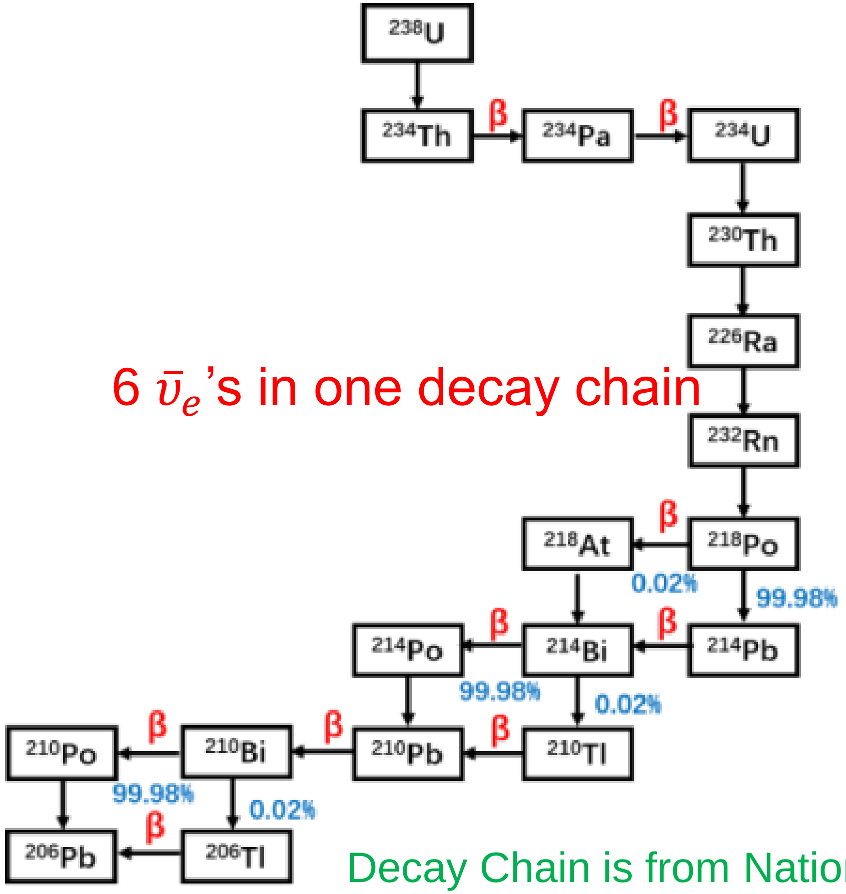

6 $\bar{\nu}_e$'s in one decay chain

Single branch calculation follows
Phys.Rev.D 100 (2019) 5, 053005
YFL, Zhang

nuclide i → nuclide j
whole decay chain

$$S_X(E_{\bar{\nu}}) = \sum_{ij} R_{ij} \sum_k I_k S_{\bar{\nu}}^{k}(E_{\bar{\nu}})$$

branch ratio

Decay information is taken from ENSDF database

Decay Chain is from National Nuclear Data Center

Geo-neutrino flux: Enomoto's flux

Normalization | Fermi function | Shape factor | Corrections

Enomoto's flux model $S^k_{\bar{\nu}}(E_{\bar{\nu}}) = K\, p_{\bar{\nu}} E_{\bar{\nu}} (E^k_0 - E_{\bar{\nu}})^2\, F(Z, E_{\bar{\nu}})\, C(E_{\bar{\nu}})\, [1 + \delta_{\bar{\nu}}(Z, A, E_{\bar{\nu}})]$

- radiative corrections
- weak magnetism
- finite size

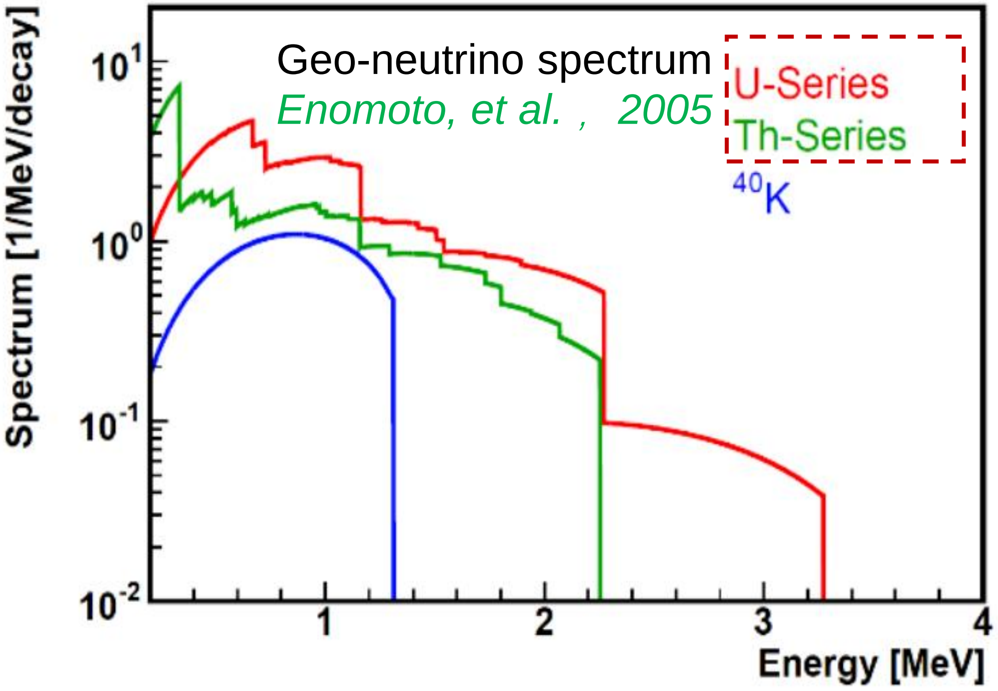

currently used in most of studies

https://www.awa.tohoku.ac.jp/~sanshiro/research/geoneutrino/spectrum/

Differences between the Enomoto's and new fluxes

	Enomoto flux	New flux
Database	ENSDF 2005	ENSDF 2023
Single branch	Only allowed transition	• forbidden decays • High order corrections

Database:

	ENSDF 2005	ENSDF 2023
$^{238}U \rightarrow {}^{208}Pb$	82 (12)	159 (12)
$^{232}Th \rightarrow {}^{206}Pb$	70 (3)	84 (3)

total transitions (effective transitions)

The extra beta branches are concentrated in the low-energy region, less than the IBD threshold.

Geo-neutrino flux: visible transitions

$i \to j$	R_{ij}	Q-value [keV]	transition number
$^{234}\mathrm{Th} \to {}^{234}\mathrm{Pa}$	1.0000	199.5	5 (0)
$^{234}\mathrm{Pa^m} \to {}^{234}\mathrm{U}$	0.9984	2290.0	24 (1)
$^{214}\mathrm{Pb} \to {}^{214}\mathrm{Bi}$	0.9998	1018.0	7 (0)
$^{214}\mathrm{Bi} \to {}^{214}\mathrm{Po}$	0.9998	3269.0	70 (6)
$^{210}\mathrm{Pb} \to {}^{210}\mathrm{Bi}$	1.0000	63.5	2 (0)
$^{210}\mathrm{Bi} \to {}^{210}\mathrm{Po}$	0.9999	1161.5	1 (0)
$^{234}\mathrm{Pa} \to {}^{234}\mathrm{U}$	0.0016	1247	39 (0)
$^{218}\mathrm{Po} \to {}^{218}\mathrm{At}$	0.0002	264.0	1 (0)
$^{206}\mathrm{Tl} \to {}^{206}\mathrm{Pb}$	0.0001	1532.3	3 (0)
$^{210}\mathrm{Tl} \to {}^{210}\mathrm{Pb}$	0.0002	4386.0	7 (5)

TABLE IV: Beta decay transitions in the ^{238}U chain. For each transition, the weight of the production ratio R_{ij}, the Q-value, and the number of decay branches are provided. The last column lists the total number of decay branches as well as the effective decay branches that can be detected by the IBD reaction.

$i \to j$	R_{ij}	Q-value [keV]	transition number
$^{228}\mathrm{Ra} \to {}^{228}\mathrm{Ac}$	1.0000	39.5	4 (0)
$^{228}\mathrm{Ac} \to {}^{228}\mathrm{Th}$	1.0000	2076.0	55 (2)
$^{212}\mathrm{Pb} \to {}^{212}\mathrm{Bi}$	1.0000	569.1	3 (0)
$^{212}\mathrm{Bi} \to {}^{212}\mathrm{Po}$	0.6406	2251.5	7 (1)
$^{208}\mathrm{Tl} \to {}^{208}\mathrm{Pb}$	0.3594	1801.3	15 (0)

TABLE V: Beta decay transitions in the ^{232}Th chain. For each transition, the weight of the production ratio R_{ij}, the Q-value, and the number of decay branches are provided. The last column lists the total number of decay branches as well as the effective decay branches that can be detected by the IBD reaction.

Geo-neutrino flux: visible branches

decay chains	$i \to j$	$R_{i,j}$	Q-value [keV]	$I_{ij,k}$	$\delta I_{ij,k}$	Transition type
^{238}U	$^{234}Pa^{m} \to {}^{234}U$	1.0000	2290.0	0.9757	0.0004	1^{st} forbidden $(0^- \to 0^+)$
	$^{214}Bi \to {}^{214}Po$	0.9998	3269.0	0.192	0.004	1^{st} forbidden $(1^- \to 0^+)$
			2660.0	0.0055	0.0008	1^{st} forbidden $(1^- \to 2^+)$
			2254.0	0.00079	0.00013	3^{rd} forbidden $(1^- \to 4^+)$
			1994.0	0.0006	0.0004	2^{nd} forbidden $(1^- \to 3^-)$
			1891.0	0.0722	0.0008	1^{st} forbidden $(1^- \to 2^+)$
			1854.0	0.009	0.0005	1^{st} forbidden $(1^- \to 0^+)$
	$^{210}Tl \to {}^{210}Pb$	0.0002	4386.0	0.20	Unknown	Allowed $(5^+ \to 4^+)$
			4210.0	0.30	0.06	2^{rd} forbidden $(5^+ \to 8^+)$
			2413.0	0.10	0.03	2^{rd} forbidden $(5^+ \to 2^+)$
			2020.0	0.10	0.03	Allowed $(5^+ \to 4^+)$
			1860.0	0.24	0.05	Unknown
^{232}Th	$^{212}Bi \to {}^{212}Po$	0.6406	2251.5	0.8643	0.0012	1^{st} forbidden $(1^- \to 0^+)$
	$^{228}Ac \to {}^{228}Th$	1.0000	2076.0	0.07	0.05	Allowed $(3^+ \to 2^+)$
			1947.0	0.006	0.005	Allowed $(3^+ \to 4^+)$

TABLE VI: Effective transitions above the IBD threshold in the decay chains of ^{238}U and ^{232}Th. In addition to the R_{ij} and Q-values provided in Table IV and V, the intensity $I_{ij,k}$, its uncertainty $\delta I_{ij,k}$, and the transition type are also listed. These values are obtained from the latest ENSDF nuclear database [23].

Geo-neutrino flux update: decomposition

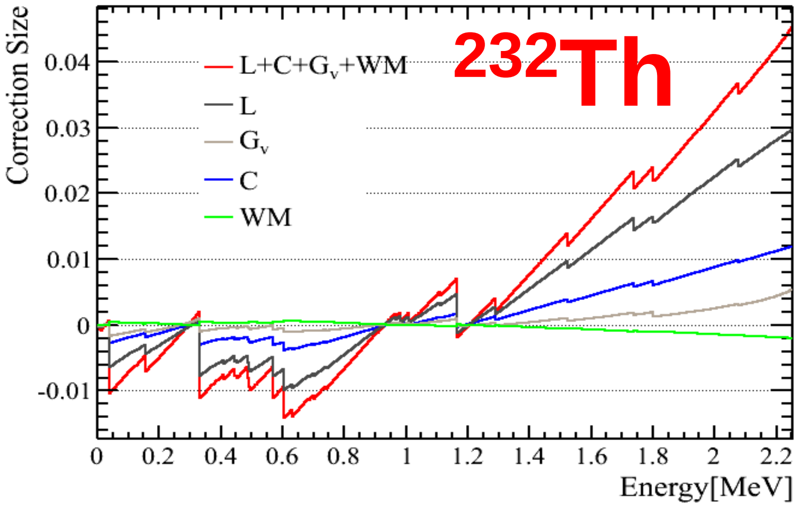

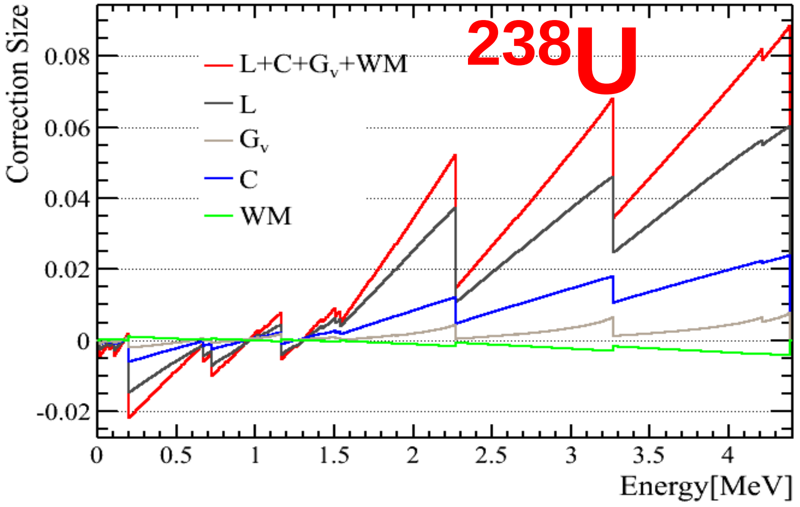

Using corrections of Huber P , (2011)

- **Corrections from:**
Finite size, radiative correction, and weak magnetism

- **Corrections from:**
Forbidden decays (shape factor)

Classification	ΔJ^π	Operator	Shape Factor $C(E_e)$		WM correction $\delta_{WM}(E_e)$
			Plane wave approximation	Exact relativistic calculation	
Allowed GT	1^+	$\Sigma \equiv \sigma\tau$	1	1	$\frac{2}{3}\frac{\mu_\nu - 1/2}{M_N g_A}(E_e\beta^2 - E_\nu)$
Nonunique first forbidden GT	0^-	$[\Sigma, r]^{0-}$	$p_e^2 + E_\nu^2 + 2\beta^2 E_\nu E_e$	$E_\nu^2 + p_e^2\tilde{F}_{p_{1/2}} + 2p_e E_\nu \tilde{F}_{sp_{1/2}}$	0
Nonunique first forbidden GT	1^-	$[\Sigma, r]^{1-}$	$p_e^2 + E_\nu^2 - \frac{4}{3}\beta^2 E_\nu E_e$	$E_\nu^2 + \frac{2}{3}p_e^2\tilde{F}_{p_{1/2}} + \frac{1}{3}p_e^2\tilde{F}_{p_{3/2}} - \frac{4}{3}p_e E_\nu \tilde{F}_{sp_{1/2}}$	$\frac{\mu_\nu - 1/2}{M_N g_A}\frac{(E_e\beta^2 - E_\nu)(p_e^2 + E_\nu^2) + 2\beta^2 E_e E_\nu (E_\nu - E_e)/3}{p_e^2 + E_\nu^2 - 4\beta^2 E_\nu E_e/3}$
Unique first forbidden GT	2^-	$[\Sigma, r]^{2-}$	$p_e^2 + E_\nu^2$	$E_\nu^2 + p_e^2\tilde{F}_{p_{3/2}}$	$\frac{3}{5}\frac{\mu_\nu - 1/2}{M_N g_A}\frac{(E_e\beta^2 - E_\nu)(p_e^2 + E_\nu^2) + 2\beta^2 E_e E_\nu (E_\nu - E_e)/3}{p_e^2 + E_\nu^2}$

$$\tilde{F}_{p_{3/2}}(E_e, R) \simeq F_1(E, Z)/F_0(E, Z) ,$$

$$\tilde{F}_{p_{1/2}}(E_e, R) \simeq \left[\left(\frac{\alpha Z}{2} + \frac{E_e R}{3}\right)^2 + \left(\frac{m_e R}{3}\right)^2 - \frac{2m_e^2 R}{3E_e}\left(\frac{\alpha Z}{2} + \frac{E_e R}{3}\right)\right] / j_1^2(p_e R)$$

$$\tilde{F}_{sp_{1/2}}(E_e, R) \simeq \left[\left(\frac{\alpha Z}{2} + \frac{E_e R}{3}\right) - \frac{m_e^2 R}{3E_e}\right] / \left(j_0(p_e R) j_1(p_e R)\right) ,$$

Stefanik, Dvornicky and Simkovic (2017)

Forbidden shape factors

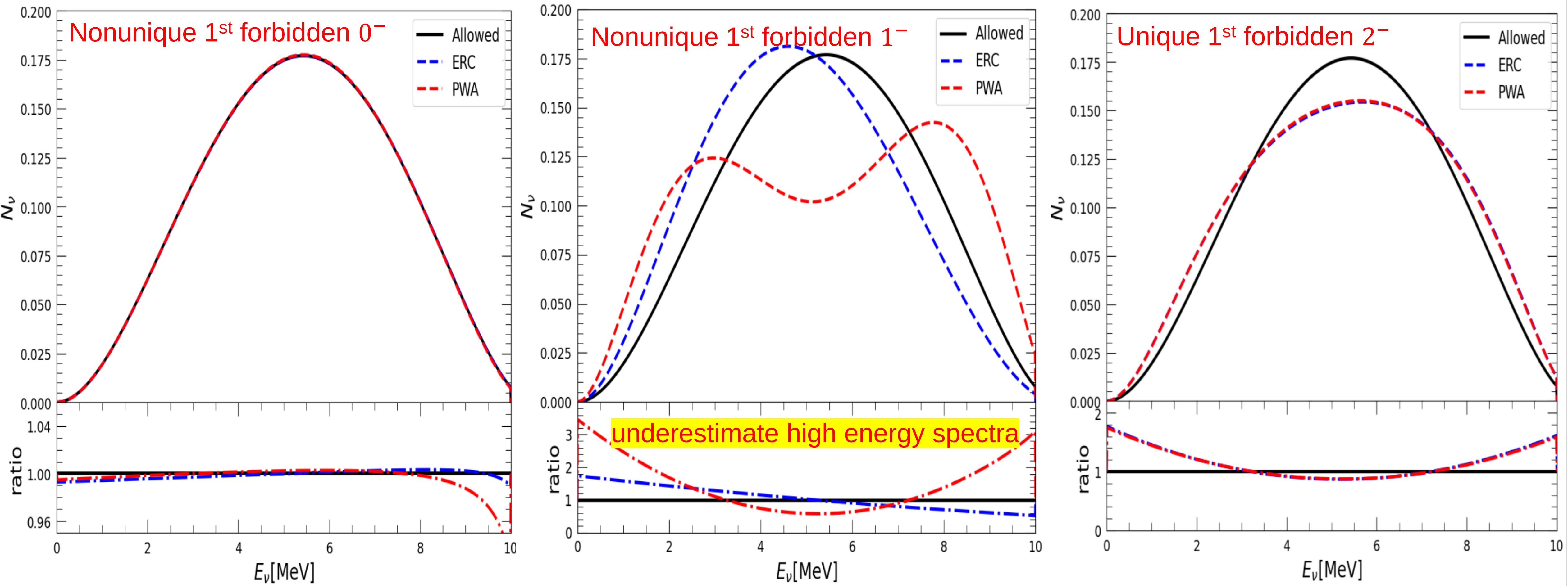

PRD 100 (2019) 5, 053005 , YFL, Zhang

We choose exact relativistic calculation (ERC) from ***Stefanik, Dvornicky and Simkovic (2017)***

ERC v.s. Microscopic calculations

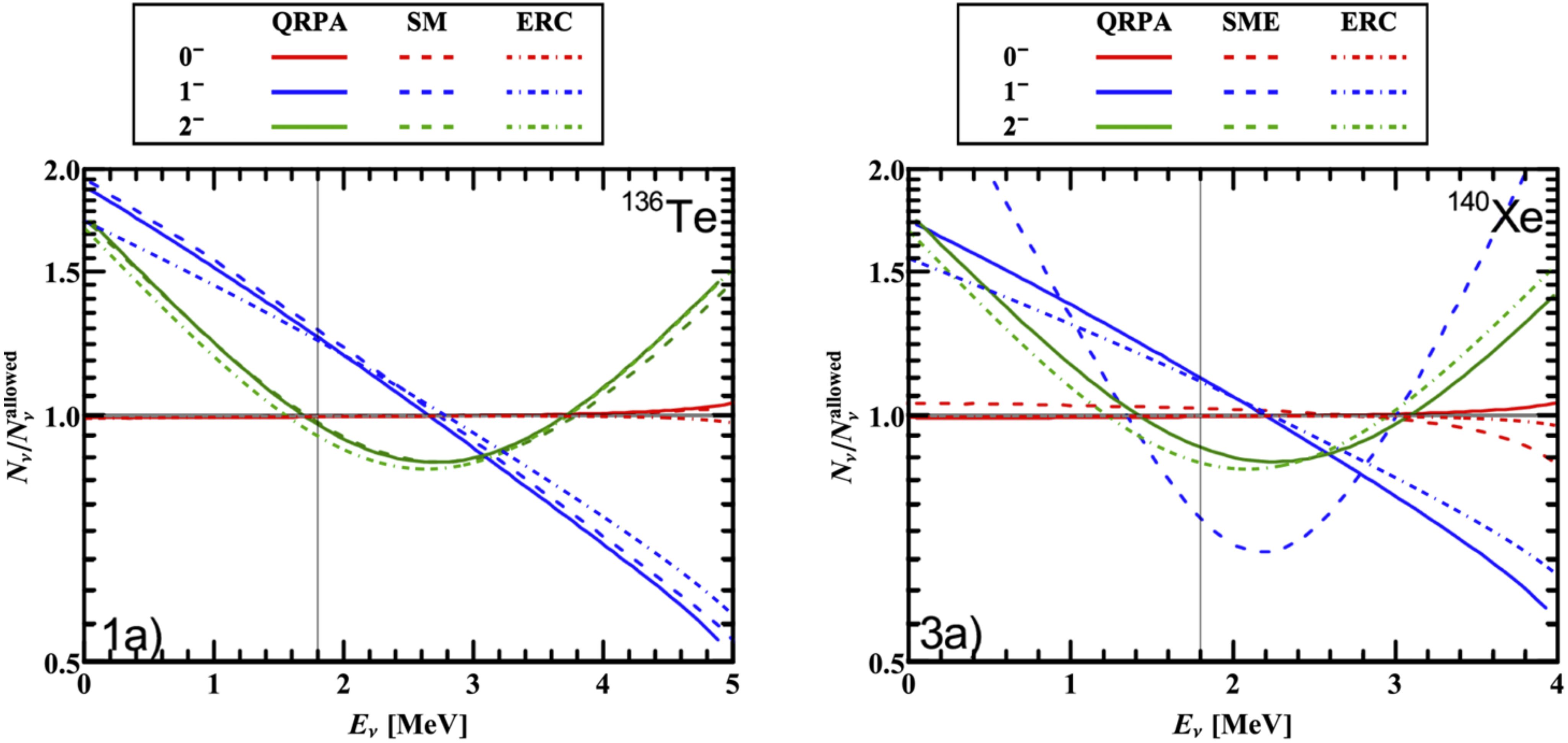

Here QRPA and SM microscopic calculations are from Fang & Brown (2015)

Phys.Rev.C 91 (2015) 2, 025503

Updated flux: update on database

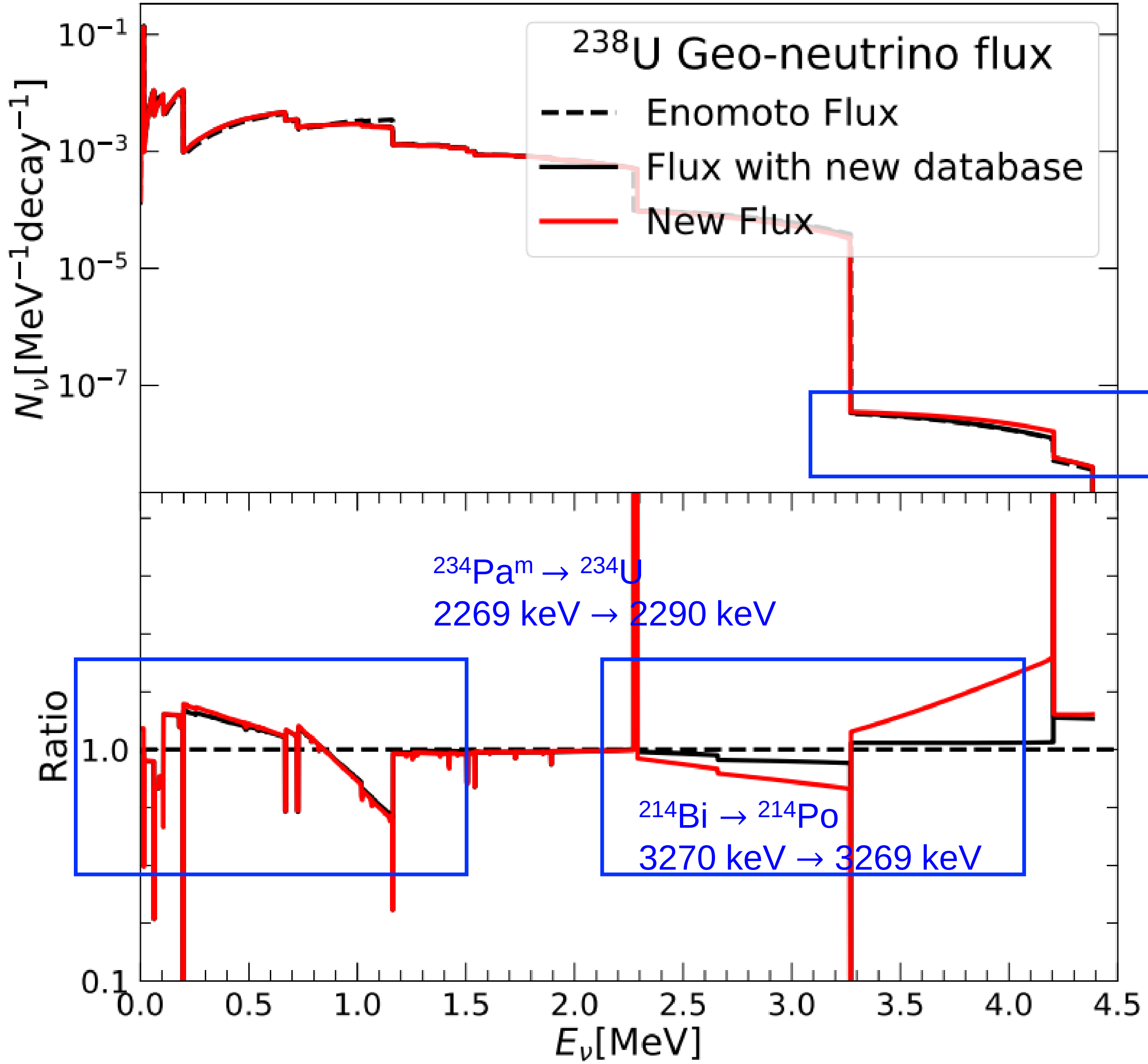

Flux with new database: calculated with ENSDF 2023

New flux: calculated with ENSDF 2023 + Forbidden decays + Higher-order corrections

^{210}Tl → ^{210}Pb not observed in neutrino experiments yet

- The extra beta branches in low-energy region
- Forbidden decays
  - ^{214}Bi → ^{214}Po 1st non-unique forbidden ($\Delta J^{\pi} = 1^{-}$)
  - ^{234}Pa^{m} → ^{234}U 1st non-unique forbidden ($\Delta J^{\pi} = 0^{-}$)

Updated flux: update on database

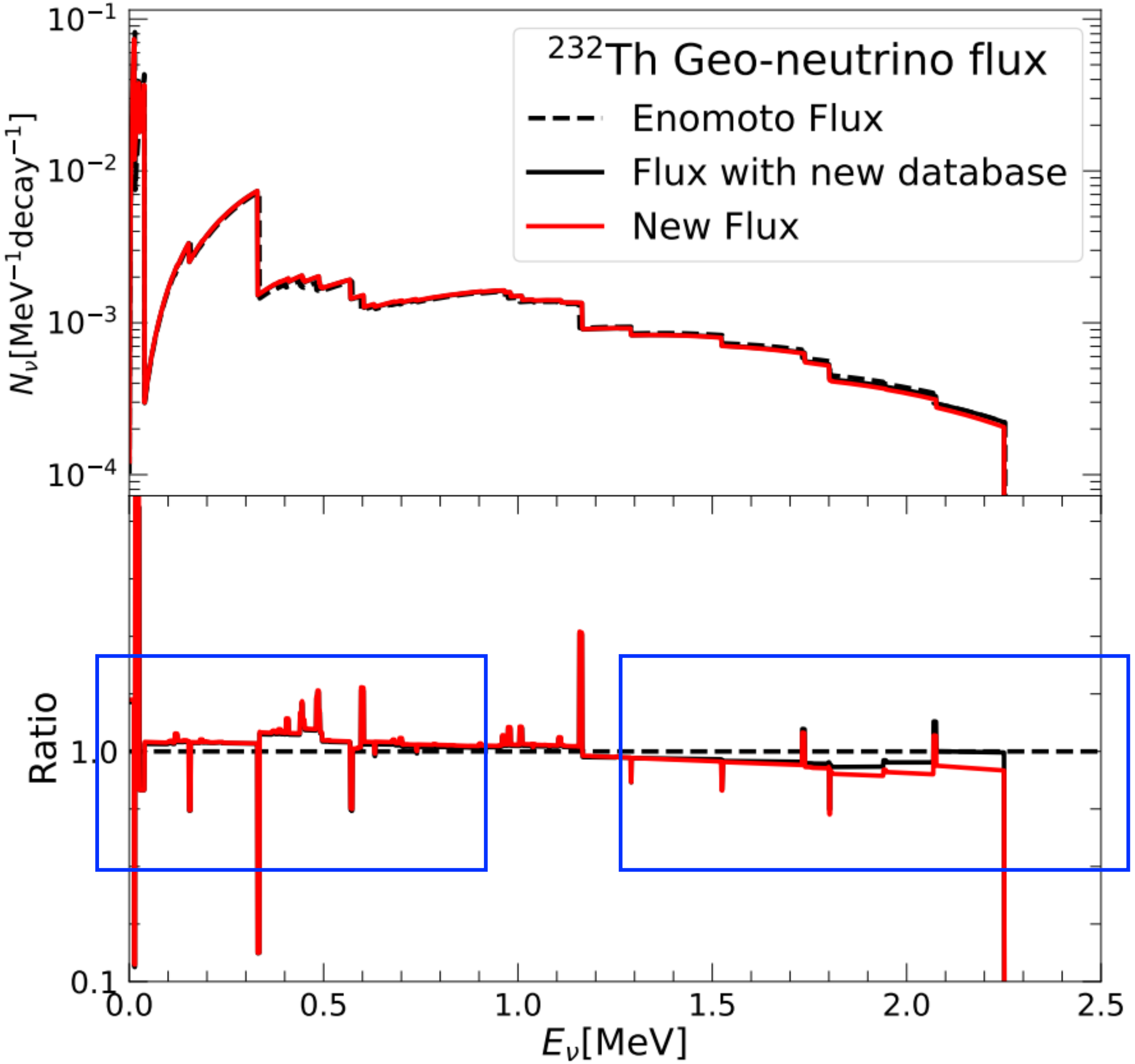

Flux with new database: calculated with ENSDF 2023

New flux: calculated with ENSDF 2023 + Forbidden decays + High-order corrections

- The extra beta branches in low-energy region
- Forbidden decays
  ^{212}Bi $\rightarrow ^{212}$Po 1st non-unique forbidden ($\Delta J^\pi = 1^-$)

Prediction with IBD cross section

R_i means the event rates for different flux models (used $\langle P_{ee}\rangle$) is detected by σ_{SV}^{rc}

$$(R_{New} - R_{Enomoto})/R_{Enomoto}$$

	Database	forbidden decay+database
^{232}Th	-3.88 %	-9.00%
^{238}U	+0.16 %	-3.47%

Enomoto flux

Updated flux

$\langle P_{ee}\rangle$ →

Strumia-Vissani + radiative corrections

$\boldsymbol{\sigma_{SV}^{rc}}$

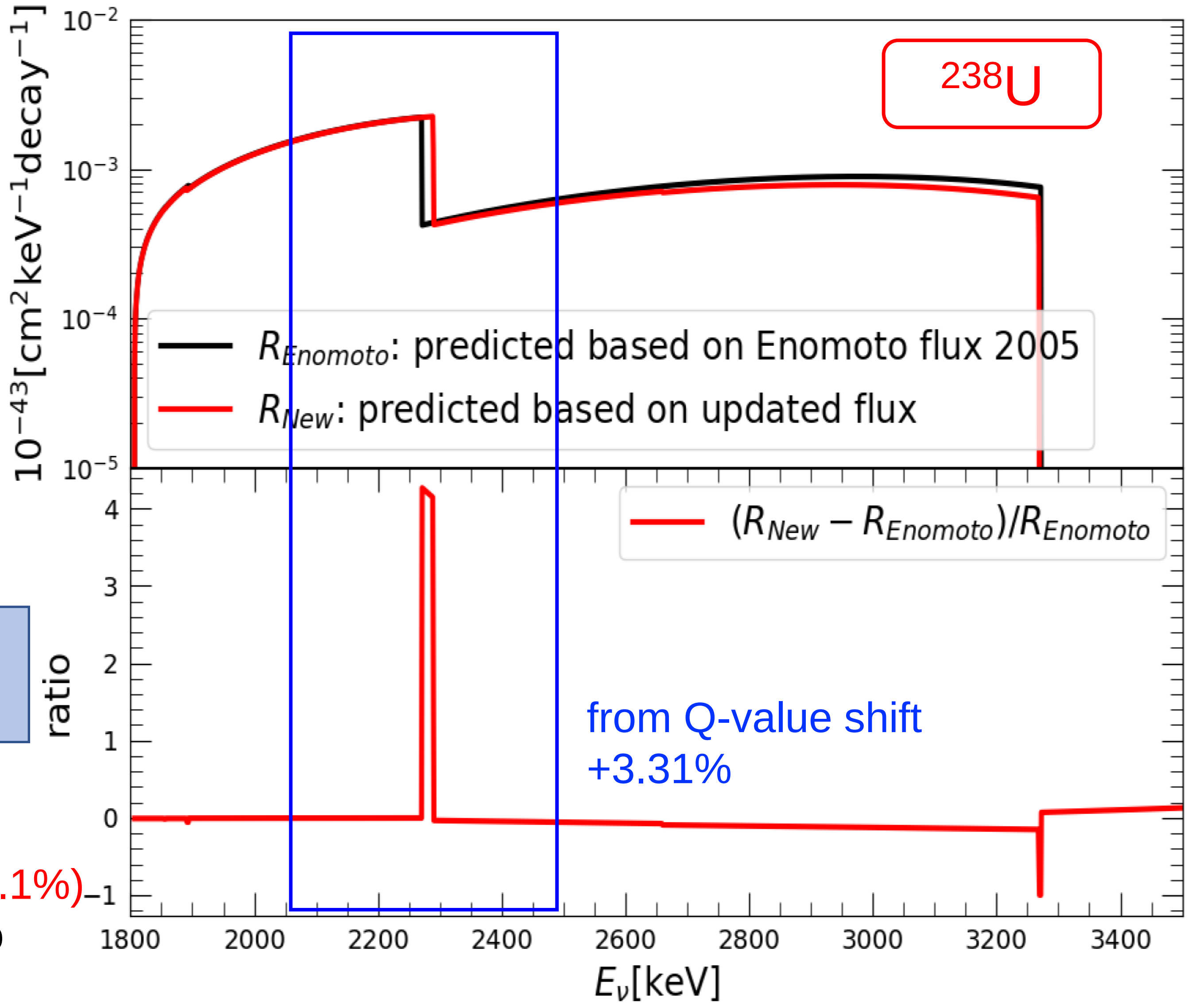

The forbidden decays will bring additional ~ -3.6% (-5.1%) for ^{238}U (^{232}Th) geoneutrino estimation for geoneutrino event numbers.

The impact on the current and future exps.

Observation in KamLAND & Borexino

KamLAND (2022)

- Liquid scintillator of 1 kon
- 18 years ~ 170 geo-neutrinos
- Precision
  - ~ 36% for ^{238}U
  - ~ 53% for ^{232}Th

Geophysical Research Letters, 49, e2022GL099566

Borexino (2020)

- Liquid scintillator of 0.3 kon
- 10 years ~ 50 geo-neutrinos
- Precision
  - ~ 53% for ^{238}U
  - ~ 55% for ^{232}Th

Phys. Rev. D 101, 012009 (2020)

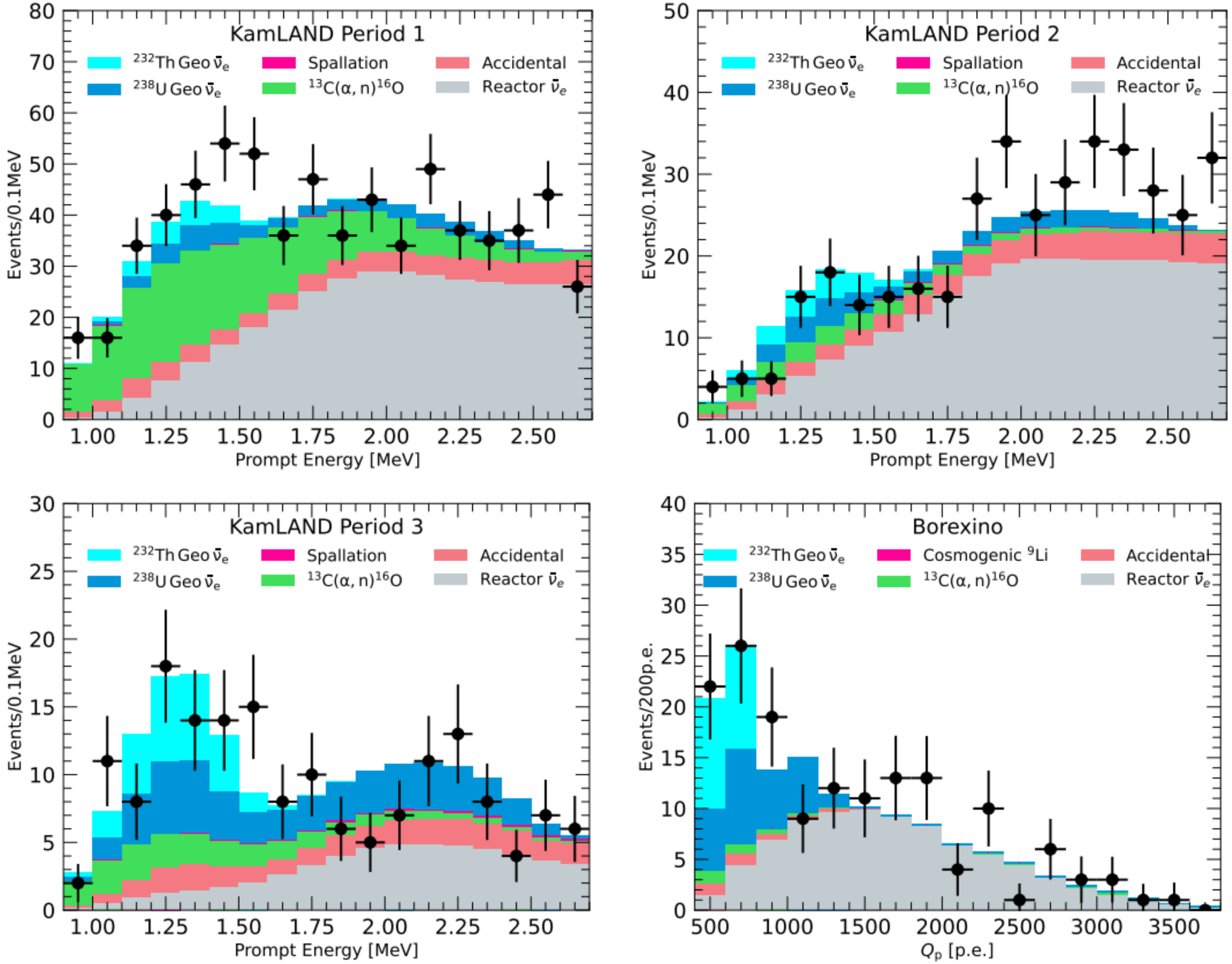

Impact on KamLAND and Borexino

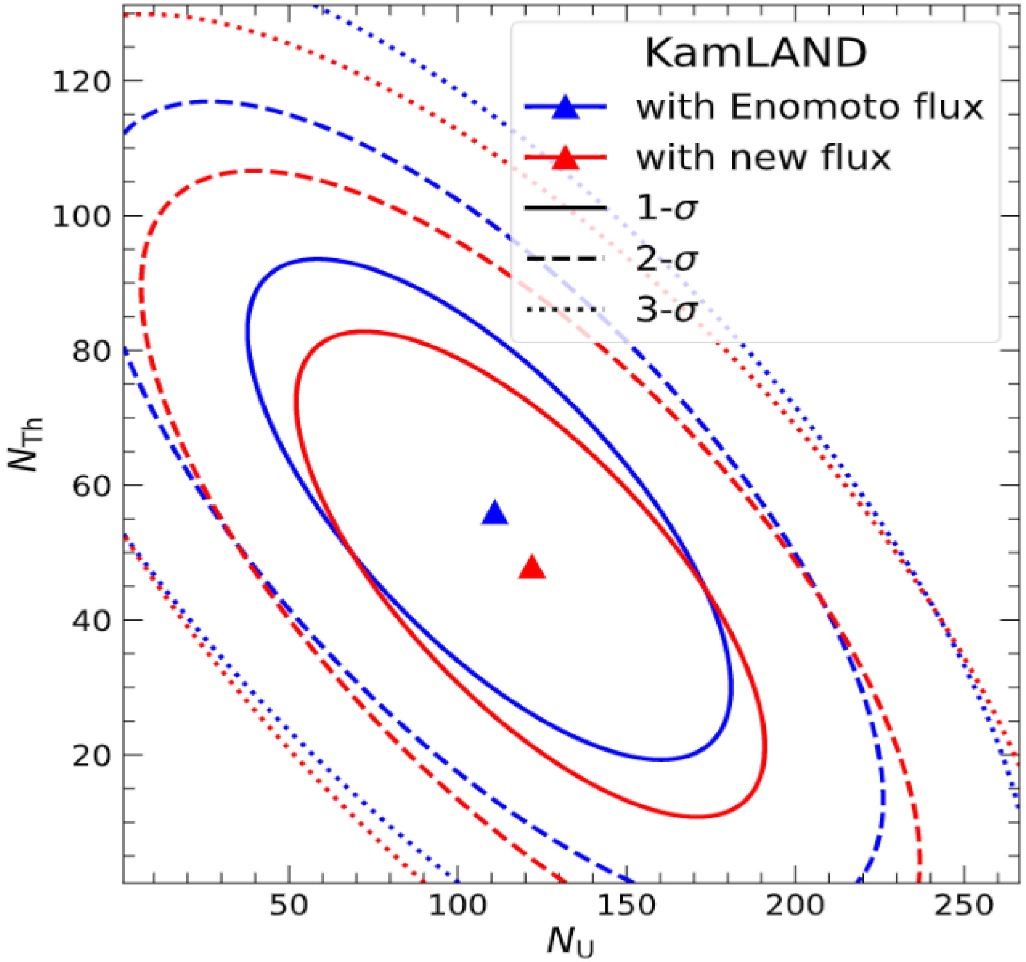

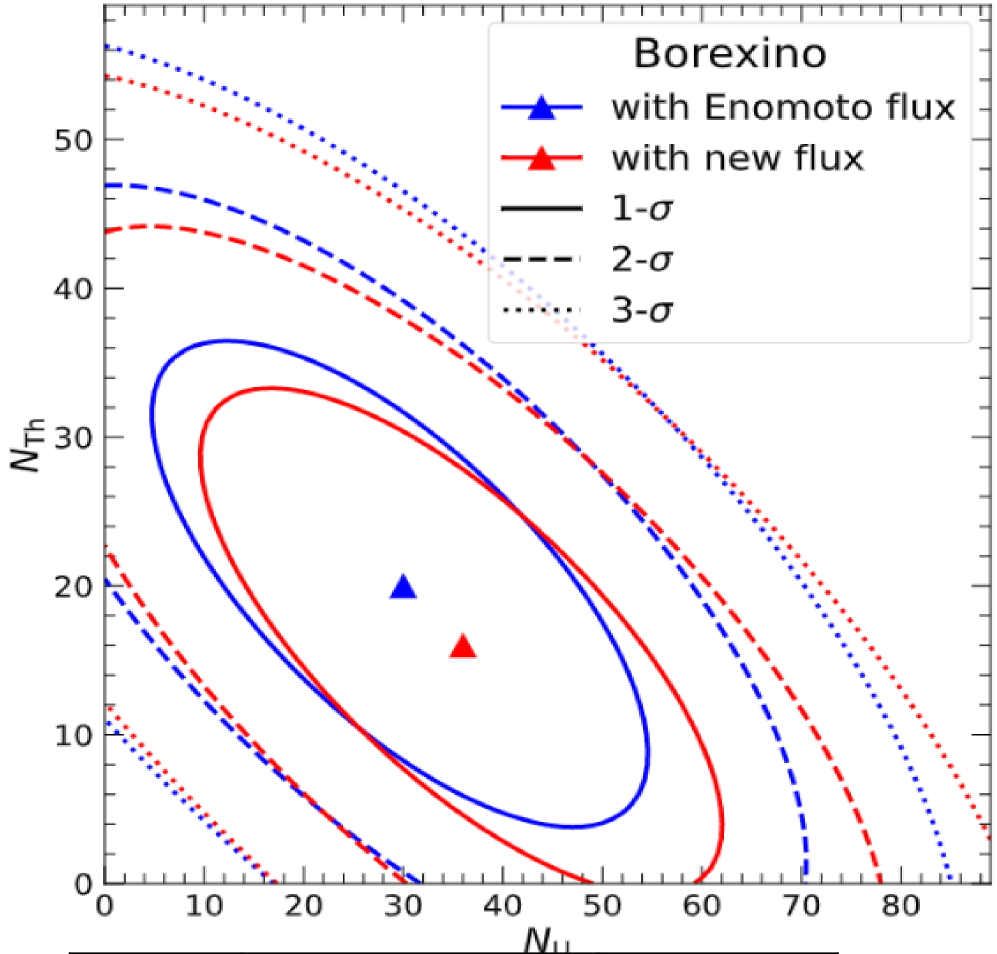

	Enomoto's flux	New flux	
N_{238}	111 ± 40 (**36%**)	122 ± 40	**+10% (0.3σ deviation)**
N_{232}	56 ± 30 (**53%**)	48 ± 28	**−16% (0.4σ deviation)**

	Enomoto's flux	New flux	
N_{238}	30 ± 16 (**53%**)	36 ± 17	**+18% (0.4σ)**
N_{232}	20 ± 11 (**55%**)	16 ± 11	**−22% (0.2σ)**

Observation in JUNO

Talk this morning!

Geo-neutrino signals
- From the decay chains of ^{232}Th and ^{238}U
- About 1 event per day

Reactor neutrinos
- contributed by two near NPPs (52.5 km) and Daya Bay NPP (~200 km)

Neutrino selection efficiency: **82.2%**

	Rate [cpd]	Rate uncert.	Shape uncert.
Geo-neutrinos	1.2	-	5%
Reactor neutrinos	47.1	-	Daya Bay/ TAO
Accidental	0.8	1%	-
$^{9}Li/^{8}He$	0.8	20%	10%
$^{13}C(\alpha, n)^{16}O$	0.05	50%	50%
Fast neutron	0.1	100%	20%
World reactor neutrinos	1	2%	5%
Atmospheric neutrinos	0.16	50%	50%

World reactor neutrinos
- contributed by the NPPs (>300km)

JUNO will measure in 1y ~400 geo-neutrinos events more than Borexino and KamLAND in >10y!

Chin.Phys.C 46 (2022) 12, 123001

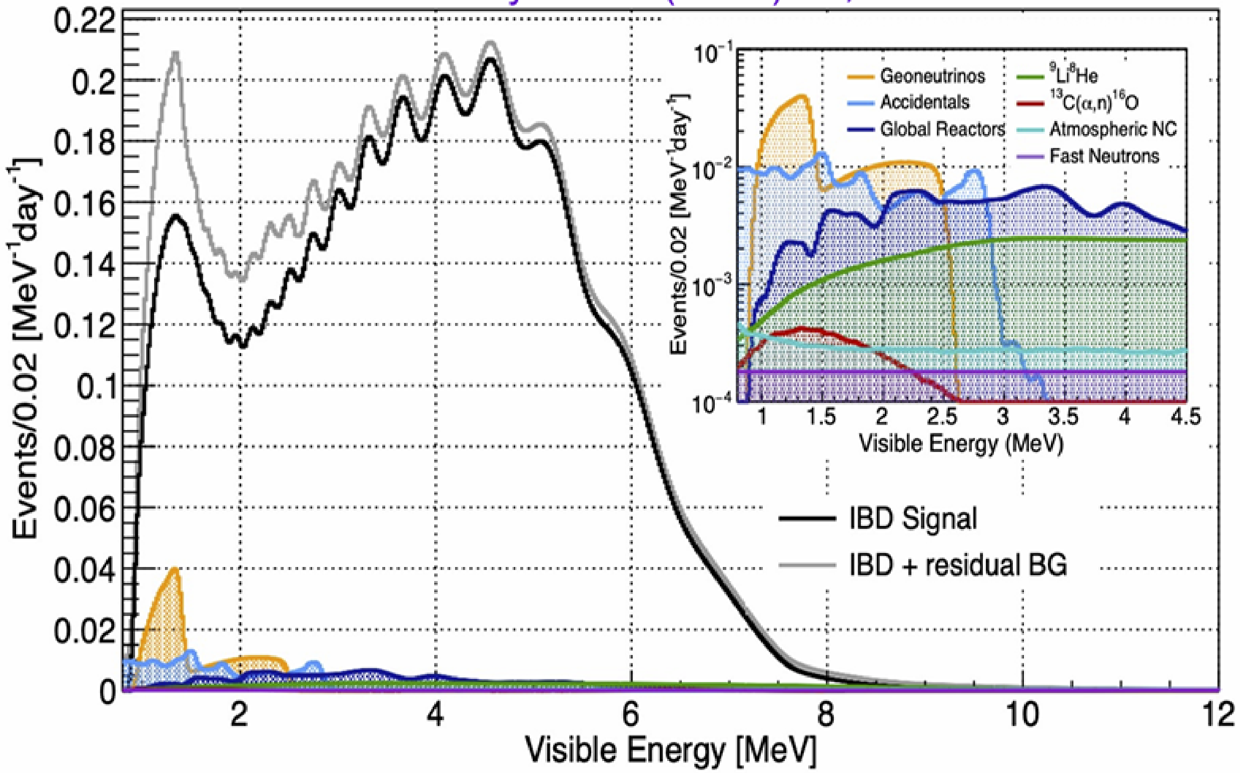

JUNO Analysis (preliminary)

- Current observation predicted with **Enomoto's flux**
- Fitted with **Enomoto's**

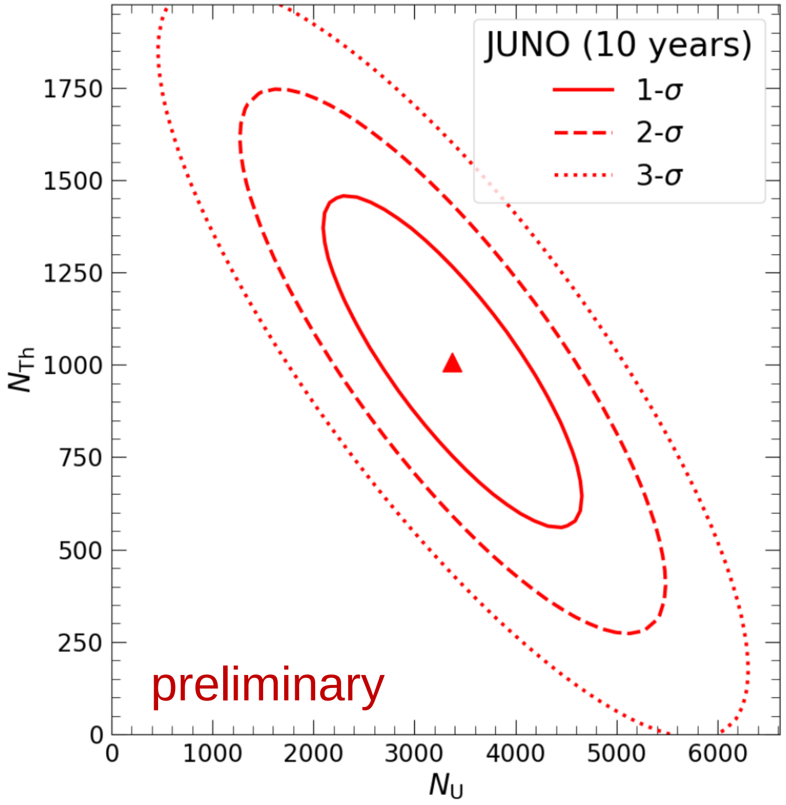

- Assuming observation predicted with **new flux**
- Fitted with **Enomoto's and new fluxes**, respectively

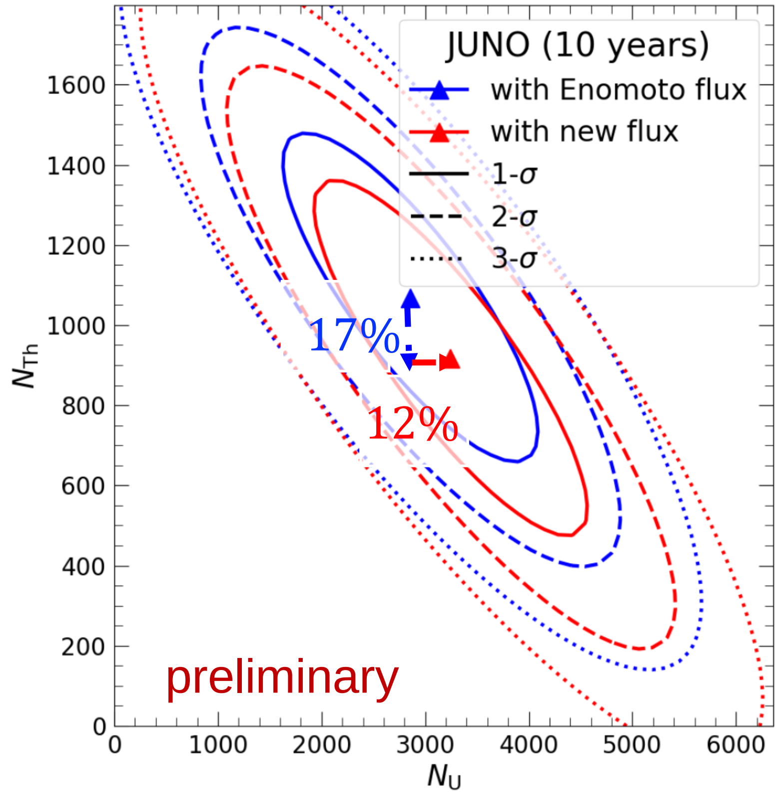

Central value: bias
Relative uncert.

	Data: Enomoto	Fit: Enomoto
N_{238}	3375	3375 ± 864 (~25%)
N_{232}	1008	1008 ± 304 (~30%)

	Data: New Flux	Fit: New Flux	Fit: Enomoto
N_{238}	3258	3258 ± 900 (27.6%)	2868 ± 746 (26.0%)
N_{232}	917	917 ± 321 (35.0%)	1068 ± 346 (32.4%)

JUNO Analysis (preliminary)

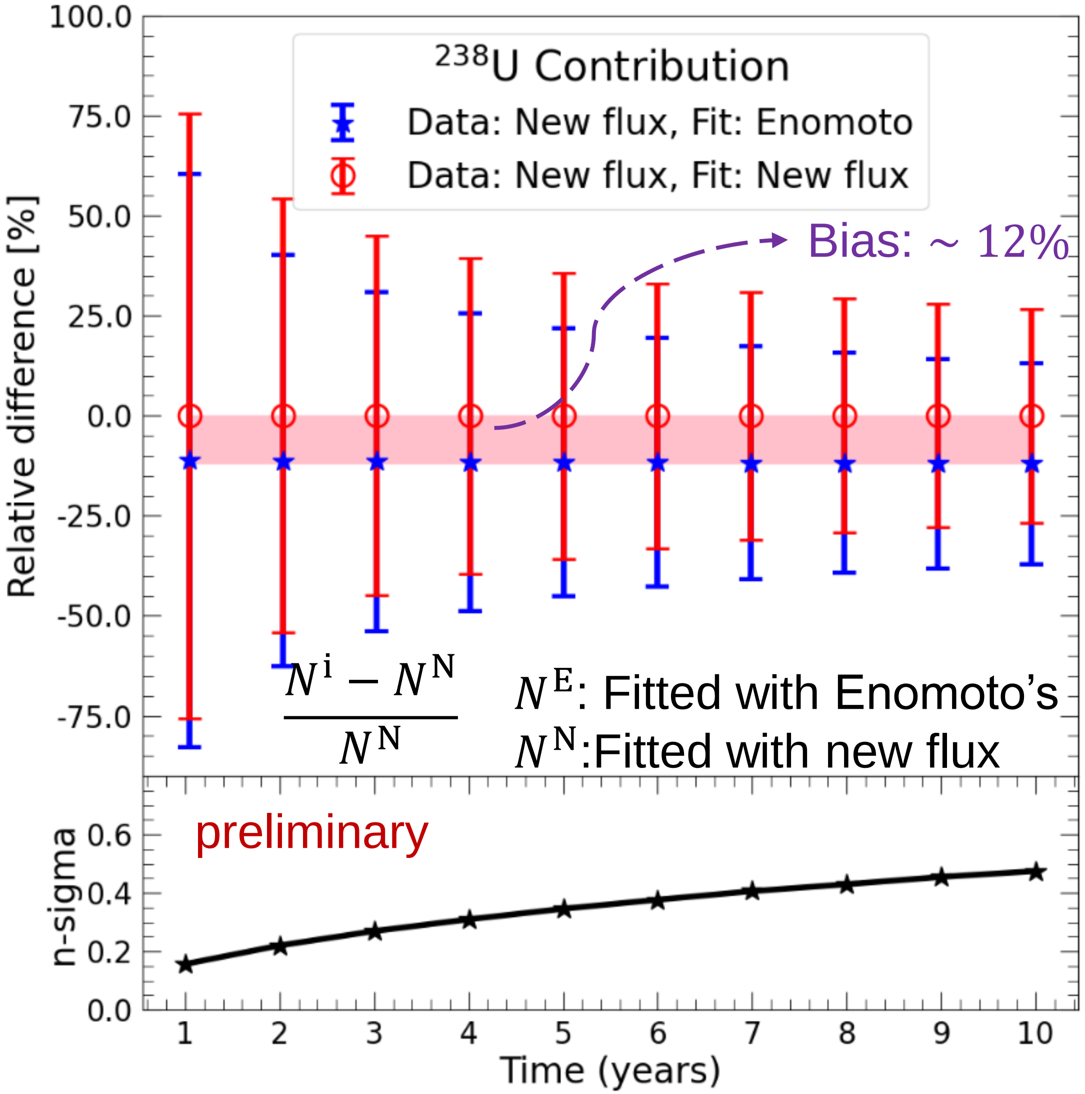

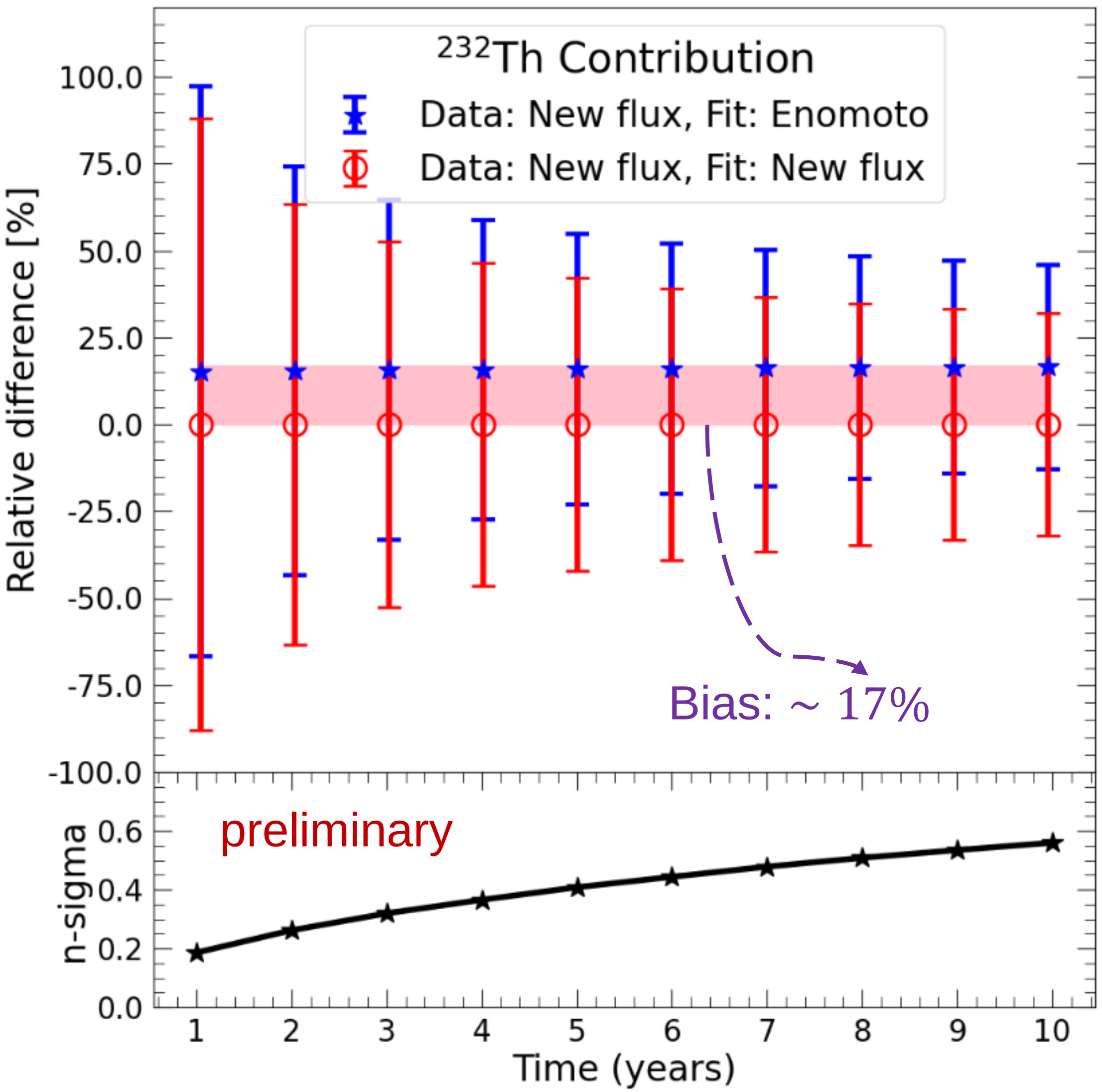

The relative bias is unchanged while the significance will be enlarged.

JUNO Analysis (preliminary)

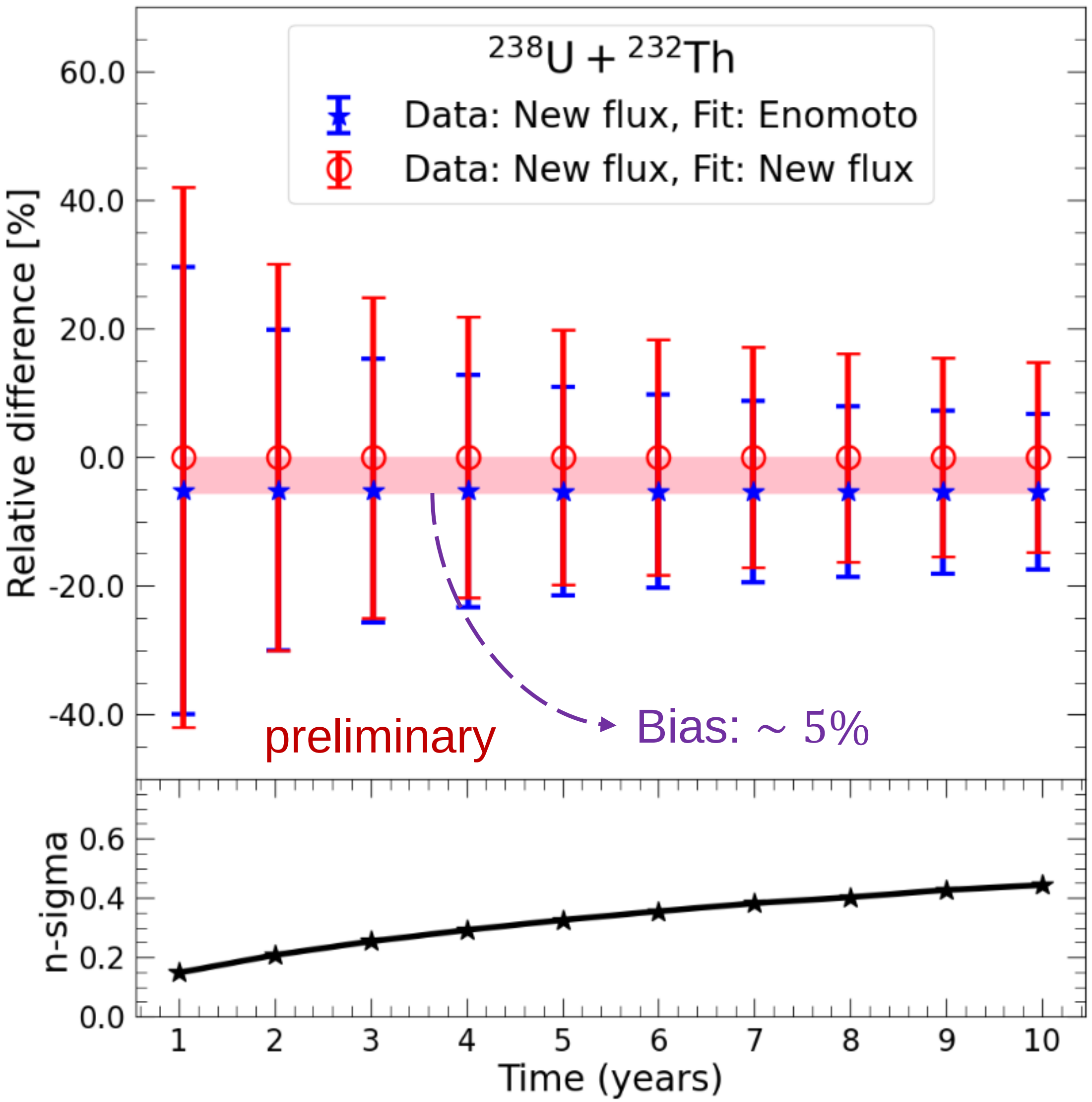

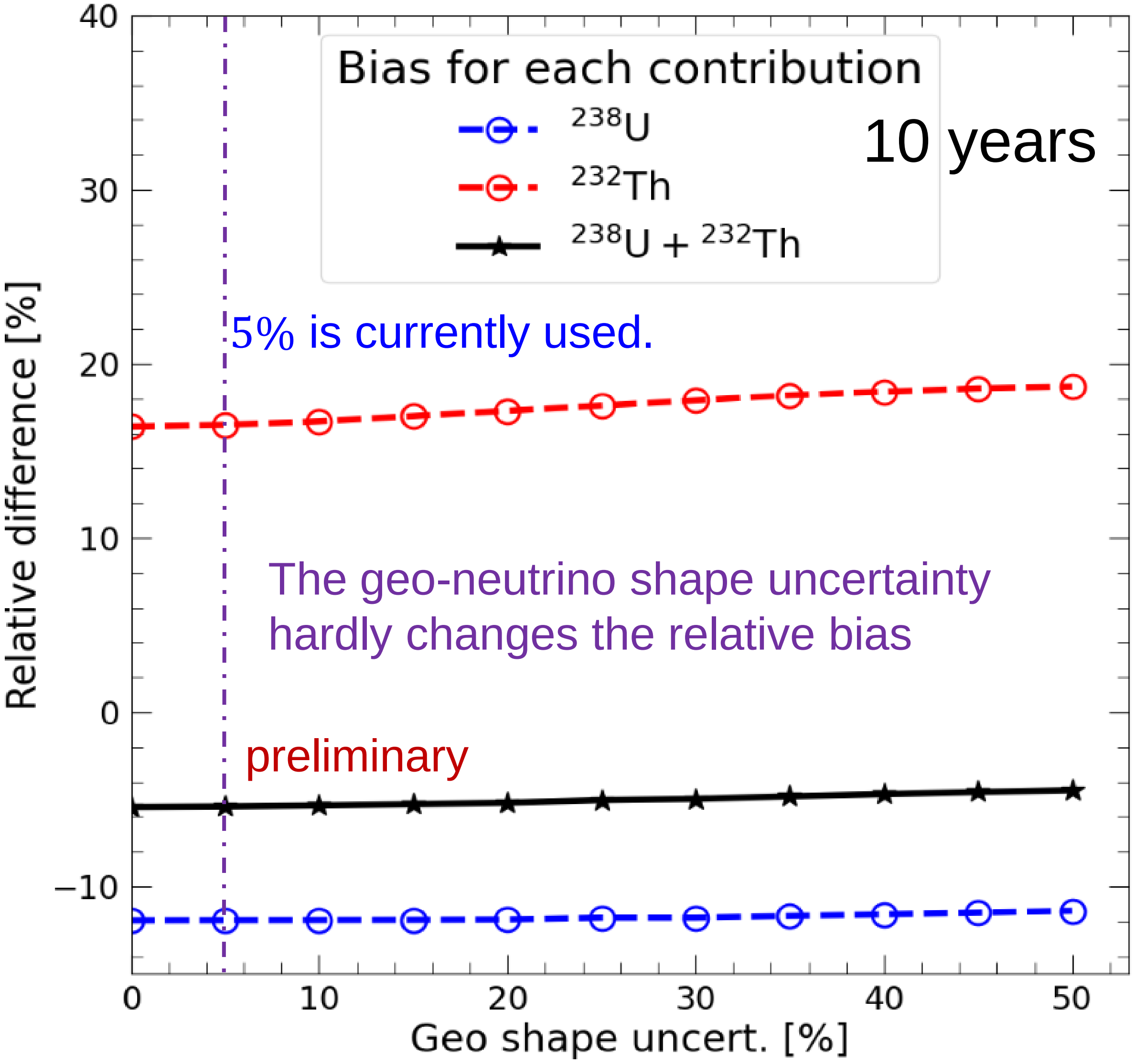

Conclusion

- ➢ A new geoneutrino flux model is presented.
  - based on new nuclear database: ENSDF 2023
  - including higher order corrections & forbidden decays
- ➢ IBD yields: ~10%, significant shape variation at high energy range
  - A Q value shift of 21 keV ($^{234}Pa^m \to {}^{234}U$): 3.3%
- ➢ Forbidden shape factor is validated with microscopic calculations
  - → **Uncertainty evaluation**
  - → **Direct measurements of Bi214/Bi212 at high energy range!**

- Fitting with Enomoto's flux will lead to bias to the central value comparing with the new flux model.

  The relative bias almost keeps constant
  - $\sim 10\% - 20\%$ for ^{238}U and ^{232}Th
  - $\sim 5\% - 10\%$ for $^{238}U + ^{232}Th$
  - Hardly changed by increasing geo shape uncertainty

  The significance of the bias
  - $\sim 0.5\sigma$ for current data

- ➢ New geo flux model → decrease the precision of geo signals

Thanks for your attention!

Backup